1

The Mechanistic Understanding of the Importance of Molecular Motions to Aggregation-induced Emission

Junkai Liu[1] *and Ben Zhong Tang*[1,2,3]

[1] *Department of Chemistry, Hong Kong Branch of Chinese National Engineering Research Center for Tissue Restoration and Reconstruction and Institute for Advanced Study, The Hong Kong University of Science and Technology, Clear Water Bay, Kowloon, Hong Kong, China*
[2] *Shenzhen Institute of Aggregate Science and Technology, School of Science and Engineering, The Chinese University of Hong Kong, Shenzhen, 2001 Longxiang Boulevard, Longgang District, Shenzhen City, Guangdong 518172, China*
[3] *State Key Laboratory of Luminescent Materials and Devices, Guangdong Provincial Key Laboratory of Luminescence from Molecular Aggregates, Center for Aggregation-Induced Emission, South China University of Technology, Guangzhou, China*

COPYRIGHTED MATERIAL

1.1 Introduction

Molecular motions drive most natural processes, ranging from the formation and annihilation of astronomical objects to the metabolism of microbes. All kinds of intra- or intermolecular interactions induce molecular motions in specific forms, through which the energy is generated and transformed. Mechanistic understanding and manipulation of molecular motions can lead to the effective design of smart molecular systems to achieve programmed tasks, as well as dynamic control of multiple processes. Indeed, by employing the light as a stimulus, researchers have developed a variety of functional molecular machines (e.g. molecular motors, molecular switches, molecular shuttles, and supramolecular assemblies) to achieve effective control of catalysis activity and chirality transfer in various practical applications, in which the dynamic manipulation of diverse molecular motions is critical [1].

For organic luminescence processes, molecular motions also extensively affect the photophysical behaviors for organic luminophores and govern the excited-state decay pathways, including vibrational relaxation, internal conversion, intersystem crossing, kinetic quenching, etc.[2]. Upon photoexcitation, the coupled nuclear and electronic motions will drive the excited molecules to evolve through radiative and nonradiative pathways [3]. However, traditional photophysical research usually focuses on the highly rigid and conjugated molecules and investigates the targets in the gas phase or solution, in which the importance of intramolecular motions to the luminescence is less considered, and the variation of molecular motions in the solid state is often ignored [4]. In 2001, the discovery and proposal of aggregation-induced emission (AIE) triggered the research on molecular motions and photophysical studies in the aggregate or the solid state [5]. The luminogens with the AIE property (AIEgens) often show different scales of molecular motions in different phases. Vigorous intramolecular motions in the solution can nonradiatively dissipate excited-state energy and always result in weak light emission, whereas such motions can be restricted in the solid state due to the environmental constraints so that the emission can be strongly enhanced [6].

Handbook of Aggregation-Induced Emission: Volume 1 Tutorial Lectures and Mechanism Studies, First Edition.
Edited by Youhong Tang and Ben Zhong Tang.
© 2022 John Wiley & Sons Ltd. Published 2022 by John Wiley & Sons Ltd.

The restriction of intramolecular motion (RIM) has been concluded as the most widely accepted and applicable mechanism for the AIE phenomenon through numerous experimental and theoretical exploration, and the strong electron-vibration coupling (EVC) between the excited and the ground state has been revealed to be the quantum origin of the weak emission of AIEgens in the solution [3, 7]. Recently, the connotation of RIM has been further clarified with deeper mechanistic insights into various novel AIEgens. The nonadiabatic excited-state molecular dynamics [8] and theoretical model based on multiple electronic states [9] have been employed to elucidate the dynamic evolution of excited states through molecular motions of tetraphenylethylene (TPE) derivatives and heteroatom-containing AIEgens. Meanwhile, the aromaticity reversal in the excited state [10] and the anti-Kasha emission from higher excited states [11] have provided another proof for the enhanced emission efficiency in the solid state for AIEgens. Apart from the critical effect on the nonradiative decay, molecular motions have also been verified to promote the electronic transition process [12, 13]. The excited-state through-space conjugation facilitated by excited-state molecular motions has been proved to contribute to the enhanced visible light emission of a series of nonconjugated AIEgens [13].

In this chapter, we will take a journey of mechanistic studies for AIE from the general RIM to mechanisms developed recently and propose the perspective on the further exploration in the future.

1.2 Restriction of Intramolecular Motion

When we look into the AIE phenomenon, two essential questions arise: why do the AIEgens show none or weak emission in the solution? Why does the aggregation brighten the light emission of AIEgens? Enthusiastic efforts have been devoted to deciphering the AIE mechanism. Several possible mechanisms have been proposed, including intramolecular conformation planarization, J-aggregate formation, *E*/*Z* isomerization, and excited-state intramolecular proton transfer, but they are only applicable for specific molecular systems [6c]. A general working mechanism for AIE is highly desired for fundamental understanding and material designing.

Upon absorption of photons, the excited molecule will decay through radiative and nonradiative paths or the photochemical process [2]. Hence, AIEgens in the solution may mainly undergo nonradiative decay or photochemical reaction to dissipate the majority of energy. Once aggregation occurs, the nonradiative decay paths can be blocked, or the radiative paths can be facilitated so that the emission can be enhanced. As the structure determines the property, typical AIEgens own flexible structures, containing multiple rotor or vibrator substituents, like hexaphenylsilole (HPS) and TPE, which endow them with high flexibility and potential to consume energy through intensive intramolecular motion, whereas multiple intermolecular interactions exist in the aggregate state, which can serve as constraints to molecular motions detrimental to the emission [6]. Continuous experimental exploration has been made through manipulation of the molecular motions by adjusting environmental factors, including hydrophobic interaction, temperature, viscosity, pressure, host–guest interaction, and intramolecular constraints such as substituent steric hindrance, ring closing, conjugation effect, and so on [14]. With persistent effort, Tang and coworkers have proposed the restriction of intramolecular rotation (RIR), the restriction of intramolecular vibration (RIV), and, finally, concluded that the restriction of intramolecular motion (RIM) was the general working principle for AIEgens [15].

1.2.1 Restriction of Intramolecular Rotation

Investigation of the effect from molecular motions on luminescence processes has drawn increasing interests. The less conjugated structures and intrinsic steric congestions are responsible for the high conformational flexibility of AIEgens.

Taking HPS as the model AIEgen [14a] as shown in Figure 1.1, when HPS is fully dissolved in the THF solution to form the isolated molecular species, it shows almost no emission. With increasing water gradually into the dilute solution and keeping the same concentration, the HPS molecules tend to aggregate due to the hydrophobicity. When the water fraction reaches 60%, notable aggregate forms and the quantum yield of the whole system starts to increase. Further increasing the water fraction, the light emission is continuously enhanced due to the further aggregation. According to general physics, any form of motion can consume energy. When we look into the structure of HPS analyzed from the X-ray diffraction, it can be found that six phenyl rings are attached to the central silole ring through single bonds with large dihedral angles, which allow free torsion or twisting motions, indicating that motions of phenyl rings are responsible for the energy dissipation in the solution state. With increasing the solvent viscosity by adding the glycerol into the solution or decreasing the temperature of the solution from room temperature to −196 °C, the emission of HPS-2 can be gradually enhanced due to the constraints coming from the highly viscous solvent or rigidified solvent environment at the low temperature. Furthermore, introducing

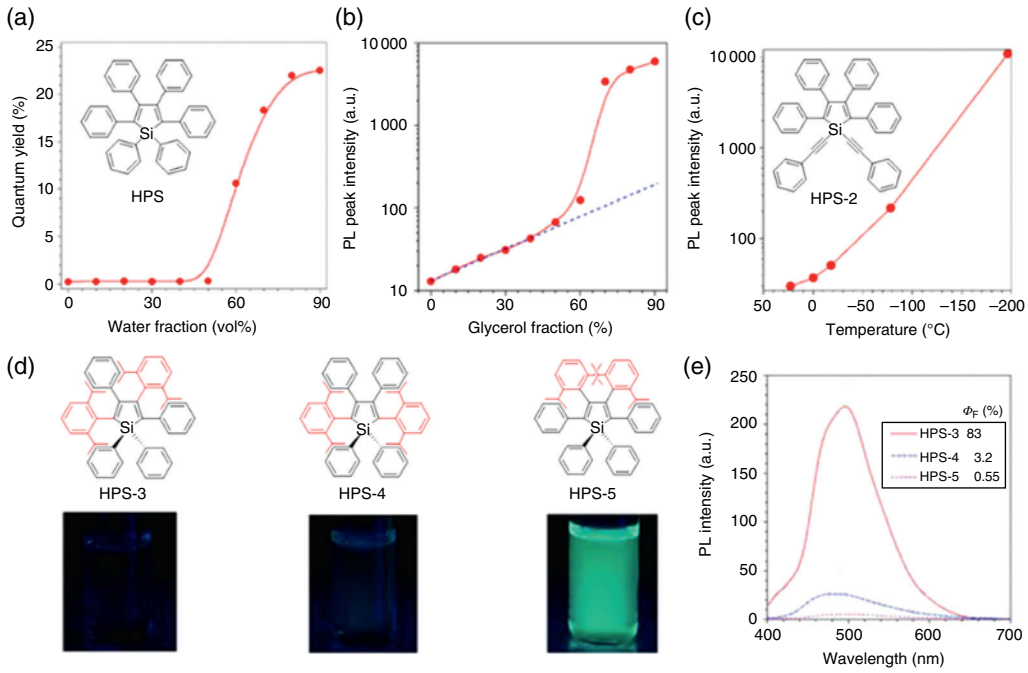


Figure 1.1 (a) Fluorescence quantum yield of HPS in the acetone/water mixtures with different water fraction. (b) Photoluminescence peak intensity of HPS in the glycerol/methanol mixtures with different glycerol fraction [HPS] = 10^{-5} M. (c) Photoluminescence peak intensity of HPS-2 in the 1,4-dioxane solution at different temperatures. [HPS-2] = 10^{-5} M. *Source:* Adapted from Ref. [14a] with permission from American Chemical Society. (d) Chemical structures and fluorescence photos. (e) Photoluminescence spectra of HPS 3–5 in the acetone solution (10^{-5} M). *Source:* Adapted from Ref. [14c] with permission from American Chemical Society.

internal steric hindrance shows a similar effect by attaching the isopropyl groups onto the 2,3,4,5-positions of the central silole as presented in Figure 1.1d and e [14c]. Crowdedness induced by the bulky groups hampers the torsion of the phenyl rings, then the nonradiative decay process can be restricted, and the emission can be restored.

TPE is another prototype of AIEgens with a similar intrinsic structure as HPS. Four phenyl rings are connected with the central double bond in a highly twisted conformation. As presented in Figure 1.3a, upon excitation, four phenyl rings can drastically twist against the double bond. Meanwhile, the C=C double bond will be weakened due to the photoexcitation, which endows it with strong twisting ability to reorganize the conformation. All these intramolecular motions result in the undetectable emission for TPE in the dilute solution. However, its emission can be dramatically boosted once the aggregation occurs. Further locking the adjacent phenyl rings through chemical bonds or attaching bulky groups onto the phenyl rings of TPE, its emission can be enhanced even in the solution [16]. All these experiments of controlling the internal or external constraints to the intramolecular motions have proved that the RIR mechanism is responsible for the AIE effect of the rotor-based AIEgens.

1.2.2 Restriction of Intramolecular Vibration

Apart from the intramolecular rotation, the intramolecular vibration in the luminogens-lacking rotors can also cause emission quenching in the dilute solution. Bu et al. have found that two coumarin derivatives fused with five-membered and seven-membered alkyl rings, respectively, show totally different photophysical behaviors, despite their similar conjugation degrees in the ground state, as indicated by the similar ultraviolet (UV)–vis absorption spectra presented in Figure 1.2 [10a].

The compound CD-5 with a five-membered ring is much more rigid and can show strong light emission in the dilute solution, but its emission is weakened in the solid, whereas the CD-7 is almost nonemissive in the dilute solution, but it can show enhanced light emission in the solid state. The calculated conformations of these two derivatives have revealed that the CD-7 with seven-membered ring owns much higher vibrational flexibility in the excited state. The central π-conjugated plane of CD-7 will suffer the vibrational motion with a dihedral angle of around 18°, so its emission can be easily quenched in the dilute solution. But such intramolecular vibration can be efficiently restricted in the solid state, which finally leads to the AIE phenomenon. The mechanism for such AIEgens-lacking rotors has been concluded as the RIV.

However, it remains unclear what the driving force is for the vigorous molecular motions on the excited state. Zhao et al. have recently systematically investigated the structure–property relationship of a series of annulene-based AIEgens and figured out the driving force of the strong vibrations in the excited state [10]. The parent cyclooctatetrathiophene (COTh) contains an eight-membered ring fused by four thiophene rings and takes a noncoplanar and saddle-like conformation as presented in Figure 1.3b. Such a highly twisted structure makes COTh nonaromatic in the ground state. The COTh shows typical AIE behavior that it can only emit negligible light in the dilute solution but shows enhanced green emission in the aggregate and solid film. The optimized structure of COTh in the ground state is similar to its single crystal structure, whereas it can relax to a transition state with a planar conformation, and finally decay through fast nonradiative pathways to the ground state. Through the calculation of the nucleus-independent chemical shift (NICS) and anisotropy of the induced current density (ACID) to characterizing the aromaticity of the structures, it has been revealed that the aromaticity reversal from the ground state to the excited

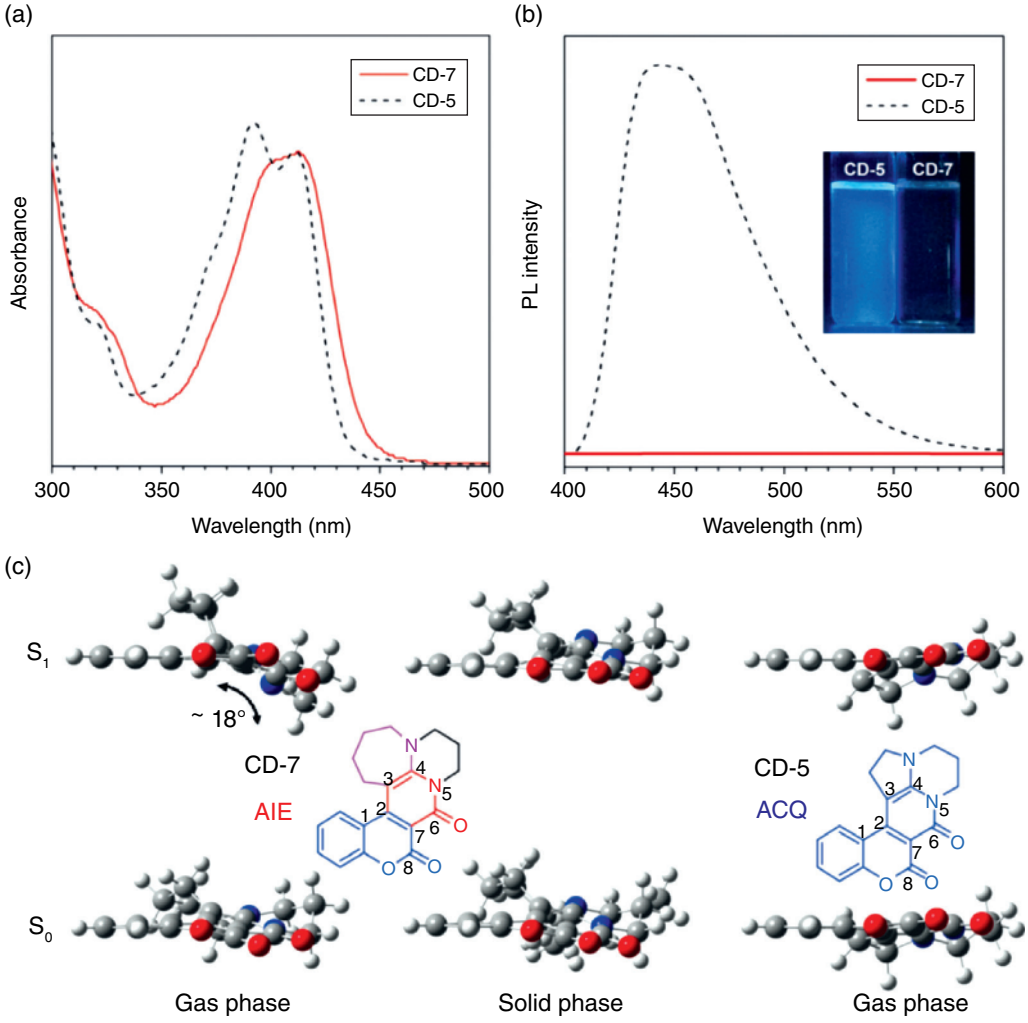


Figure 1.2 (a) UV–vis absorption and (b) photoluminescence (PL) spectra of coumarin derivative-7 (CD-7) and coumarin derivative-5 (CD-5) in CH_2Cl_2. Concentration: 10^{-5} M; excitation wavelength: 411 nm. (c) Optimized structures at the $S_{0,min}$ and $S_{1,min}$ of CD-7 in the gas and solid phases and CD-5 in the gas phase at time dependent (TD) M062X/6-31G(d) level. *Source:* Adapted from Ref. [10a] with permission from John Wiley and Sons.

state drives the conformational change through intense up–down vibration. But when the aggregation occurs, the vibration can be effectively restricted due to the environmental hindrance. Meanwhile, the energy of the planar transition state has been elevated, and the pathways to the transition state are not energetically accessible, which leads to the major radiative decay and promoted luminescence efficiency.

From the abovementioned cases, it can be concluded that RIR and RIV are the main cause of the AIE properties of propeller-shaped and shell-shaped AIEgens. Hence, the RIM can be unified as the general working principle for the AIE effect, and RIM can serve as the basic design principle for the development of AIE materials.

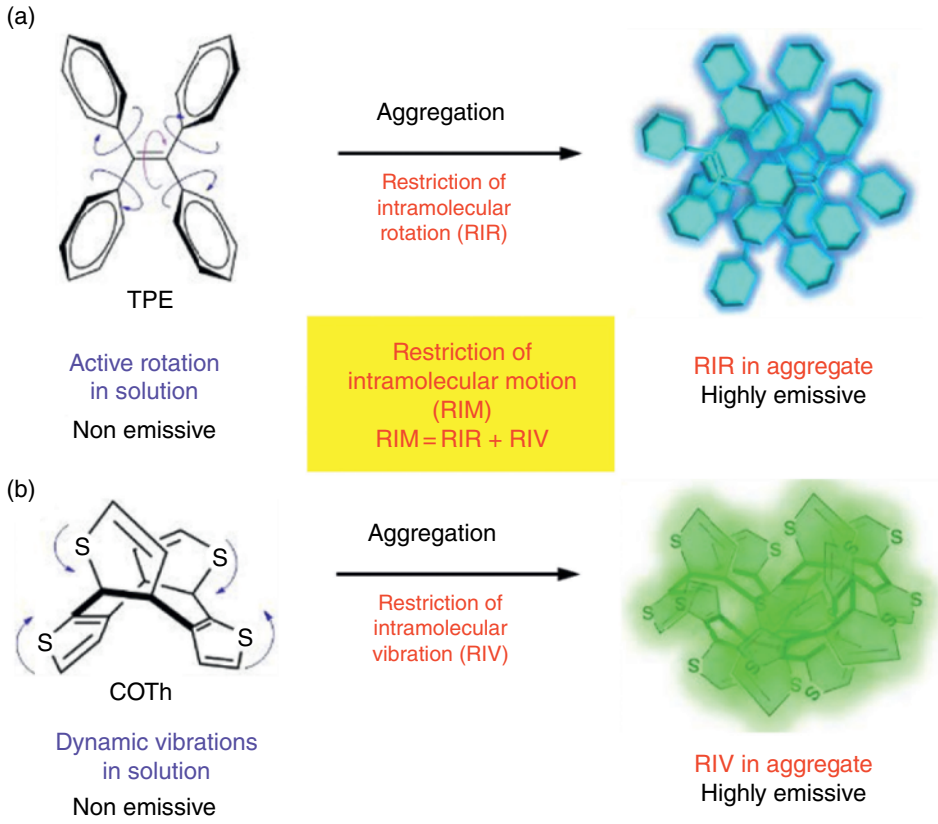


Figure 1.3 Schematic illustration of RIM mechanism. (a) Restriction of intramolecular rotation. (b) Restriction of intramolecular vibration. *Source:* Adapted from Ref. [6a] with permission from American Chemical Society and Ref. [10b] with permission from Springer Nature.

1.2.3 Ultrafast Insights into Tetraphenylethylene Derivatives

Molecular motions significantly affect the decay behaviors for AIEgens. Certain excited-state dynamics require further clarification. Tang and coworkers have developed detailed understanding of excited-state molecular motions of TPE derivatives and further elucidated the RIM mechanism through the lens of ultrafast spectroscopy [16]. As presented in Figure 1.4, six TPE derivatives with different internal constraints and structural rigidity have been prepared and studied through the first-principle calculation based on (time-dependent) density function theory ((TD)DFT) methods.

Different structural rigidities may lead to different freedom of motion and structural variation during the excited-state decay. Optimized conformations in the S_0 state and the S_1 state show that all the studied TPE derivatives undergo the elongation of the ethylenic double bond and form the quasi-double bond after excitation, but the single bonds connecting the peripheral phenyl rings with the central double bond have been shortened. These two types of bond change originate from the weakening of the double bond and the electron density flowing from the double bond to the surrounding single bonds. Meanwhile, the bond variation leads to the twisting of the quasi-double bond and the phenyl rotors.

Comparison between the S_1 and S_0 conformations shows that the parent TPE has encountered the largest structural reorganization with the torsion angle of the quasi-double bond of 56.80° and

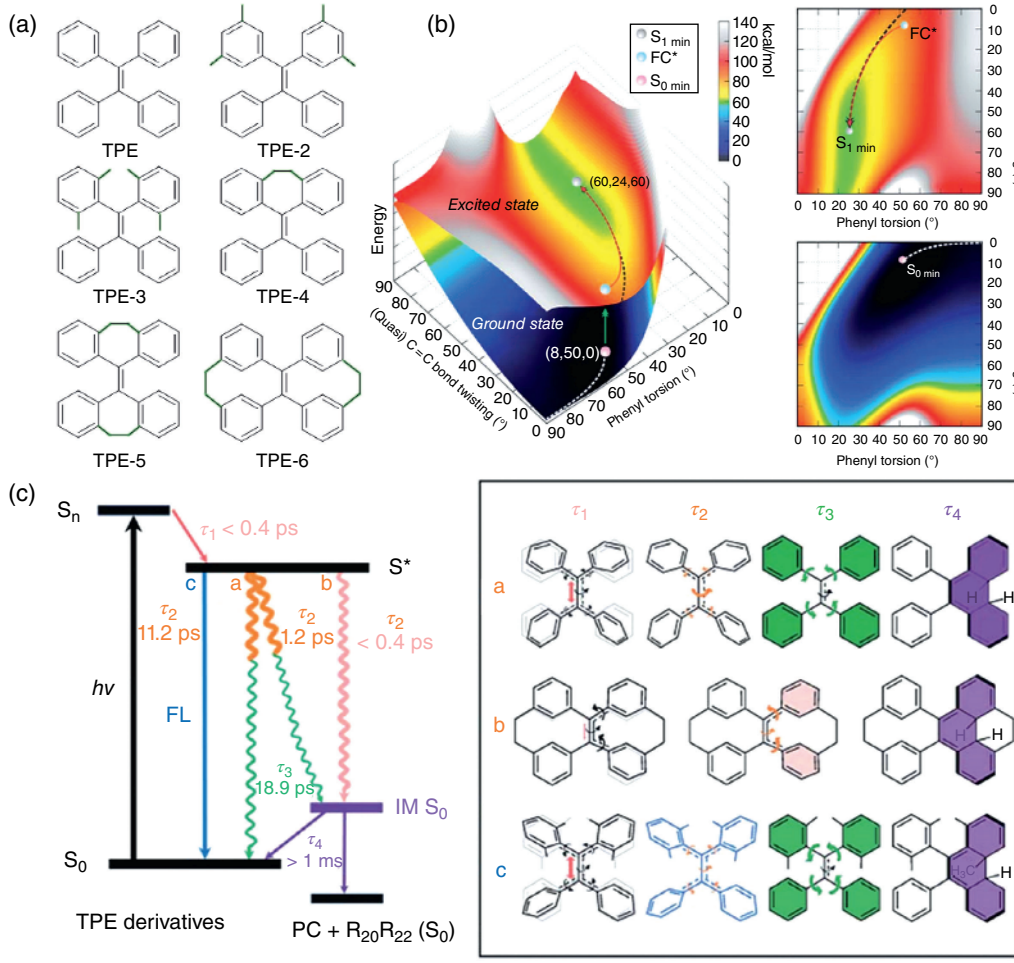


Figure 1.4 (a) Chemical structures of TPE derivatives with increasing rigidity. (b) Potential energy surfaces (PES) and projections of PES of the S_1 and the S_0 state of TPE. The MEPs on the S_1 and the S_0 state are marked as black and white dash line, respectively. (c) Schematic illustration of ultrafast excited-state decay processes of TPE derivatives and dominant molecules with different timescales. *Source:* Adapted from Ref. [16] with permission from The Royal Society of Chemistry.

the torsion angle of the phenyl ring of 29.04°, whereas with decreasing the motion freedom, derivatives show decreased structural changes. The TPE-6 with double vicinal locking of the phenyl rings only shows the double bond elongation of 0.03 Å and less than 9° twisting of the quasi-double bond. Hence, the twisting of the quasi-double bond and the torsion of the phenyl rings have been chosen as the motion coordinates to scan the potential energy surfaces (PES) of the S_1 and S_0 states. The calculated minimum energy path (MEP) in the ground state of the parent TPE is coupled by the phenyl-ring torsion from 50° to 90° and the double bond twisting of less than 9° with energy change of less than 7 kcal/mol. There is a transition state connecting two minimum points on the ground-state PES with the highly twisted quasi double bond. However, the MEP on the excited-state PES is dominantly associated with the twisting of the quasi-double bond of 50° due to the significant elongation of the original double bond of 0.12 Å, accompanied by the phenyl ring's torsion of less than 25°. The PES around the $S_{1,min}$ is shallow with the energy of 60 kcal/mol, which

is rather close to the transition state on the ground-state PES, which will lead to fast decay from $S_{1,min}$ to the ground state.

The ultrafast transient absorption spectra have further revealed the excited-state decay dynamics through the coupling of the double bond twisting and phenyl ring's torsion. For the parent TPE, upon absorption of pump light, the excited species will decay from S_n states to the S_1 state, through internal conversion within sub-picosecond, mainly associated with elongation and twisting of the C=C double bond, which can be signalized by the stimulated emission at 1.3 ps. Then, from 1.3 to 3.79 ps, the excitons populated on the emissive state revert back through twisting the quasi-double bond. After 3.79 ps, the photocyclization intermediate forms associated with the phenyl ring's torsion with an ultralong lifetime of 159 seconds. With increasing the intramolecular steric congests, TPE-2 shows similar excited-state dynamics with the parent TPE, whereas TPE-3 emits light efficiently within sub-picosecond even in the dilute solution. The transient emission at 480 nm of TPE-3 within 1.19 ps has confirmed the ultrafast population on the emissive $S_{1,min}$, which is consistent with the decrease of the peak at 477 nm on the ultrafast transient absorption spectra due to the stimulated emission between 0.63 and 1.2 ps. The population period takes a longer time as compared to the parent TPE, which indicates that the steric hindrance on the phenyl rings can slow down the twisting of the quasi-double bond and contribute to the stabilization of the emissive state. Further attaching the alkyl tethers between the geminal or vicinal phenyl rings will largely reduce freedom of motion of the phenyl rings and accelerate the formation of the photocyclization intermediate.

Hence, it can be concluded that TPE derivatives will undergo an ultrafast vibrational relaxation and populate on the $S_{1,min}$ after excitation through the coupled molecular motions of elongation and twisting of the C=C double bond as well as torsion of phenyl rings within the picosecond timescale, after which the photocyclization intermediate will be formed. The dominant time component in this relaxation varies, depending on the conformational rigidity. The increased steric hindrance or structural locking on the parent TPE will hamper the twisting of the quasi-double bond and stabilize the emissive state to generate efficient light, as in the case of TPE-3, or directly minimize the motions involving the double bond and the phenyl rings and make the photocyclization intermediate formed on the sub-picosecond timescale as in the case of TPE-6. Thus, motions involving the C=C double bond and the formation of the photocyclization intermediate are the dominant pathways for the excited-state deactivation of TPE derivatives in the solution.

1.2.4 Theoretical Insights into Restriction of Intramolecular Motion

The experimental investigation has proved that the intramolecular motions are responsible for the weak emission of AIEgens in the solution, and the aggregate environment can restrict such molecular motions and enhance the light emission. What kind of molecular motions can govern the excited-state decay pathways for AIEgens? How do the molecular motions dissipate the excited-state energy? Theoretical researchers have developed the proper modes for radiative decay rates and nonradiative decay rates based on the thermal vibration correlation function (TVCF) formalism, and precisely calculated the quantum yields in both solution state and aggregate state and finally revealed the quantum origins of the RIM mechanism [7].

Studies of the transition process between two electronic states relate to the quantum dynamics. The fluorescence and phosphorescence processes usually occur in the timescale from nanoseconds to milliseconds, while the internal conversion and intersystem crossing often occur in picoseconds or a shorter timescale. However, the current excited-state dynamic simulation can only deal with the process occurring within picoseconds, which is much faster than the luminescence process.

Hence, theoreticians usually evaluate the luminescence quantum efficiency by employing the decay rate formalism based on the Fermi golden rule [3]. The luminescence quantum yield Φ_F can be defined as $\Phi_F = k_r + k_{nr}$, in which k_r stands for the radiative decay rate and k_{nr} stands for the nonradiative decay rate. The k_r can be calculated with integration of multiple theories even for polyatomic molecular systems. The problem to evaluate the quantum yield is to precisely calculate the nonradiative decay rates, which contain more factors related to complicated molecular motion modes [3].

Traditional target molecules for the photophysical research always own highly rigid π-electron structure with large conjugation, which makes the effect of molecular motions less notable, whereas most AIEgens possess highly flexible molecular structures, allowing the high freedom of motion in the isolated state, which facilitates the nonradiative pathways to a large extent through diverse decay modes. Peng et al. have proved that calculation of internal conversion rates considering the Duschinsky rotation effect (DRE) leads to more accurate quantitative evaluation of the nonradiative decay process for the 1,2,3,4-tetraphenylbutadiene (TPBD) with AIE property since DRE describes the coupling among the multiple modes of molecular motions [7e]. Such mode mixing also significantly contributes to the nonradiative dissipation of excited-state energy as well as the intrinsic multiple molecular motions. On the other hand, the evaluation of the temperature-dependent luminescence behaviors of TPBD considering DRE produces more reliable results that are much closer to the experimental observation [7e].

Furthermore, for the fluorescence process, the nonradiative decay pathways are governed by the nonadiabatic coupling (NAC), which can be divided into nonadiabatic electronic coupling (NAEC) and EVC [7e]. The NAEC deciphers the electronic part that contributes to the nonradiative decay, and the EVC relates to the interaction between the electronic and the nuclear motions. The reorganization energy (RE) can be applied to evaluate the intensity of EVC and can offer detailed information on the structure–property relationship [17]. Through investigating NAEC and EVC, researchers have revealed the quantum origins of the energy-consuming mechanism from molecular motions. Taking HPS as the research model, its fluorescence quantum yield is only 0.30% in the dilute solution, whereas it can reach 78% in the solid film, which is 260 times as high as that in the solution. Zhang et al. have calculated the electronic structures of HPS in both isolated state and crystal state, using the combined quantum mechanics and molecular mechanics (QM/MM) method to explore the detailed working mechanism of HPS from quantum view [7a].

During the vibrational relaxation in the excited state, large conformational reorganization occurs, which mainly relates to the torsion of phenyl rotors on the 2,5-positions of the silole ring due to their high mobility in the isolated state. However, the optimized HPS in the crystal shows only minor conformational reorganization during the relaxation with almost no change in the dihedral angles of phenyl rings, which proves the RIM features in the solid state. Further, NAC analysis reveals that the distribution and total values of NAEC have no notable change before and after the aggregation occurs (Figure 1.5), indicating that the NAEC is insensitive to the aggregate environment. Nevertheless, the EVC analysis shows that many low-frequency motion modes ($\omega < 200$ cm^{-1}) of HPS exist in the isolated state, and they are mainly recognized as the torsion of phenyl rotors. The RE of these low-frequency modes is 197 meV, which occupies 40% of the total RE of the whole system. Afterwards, the RE of low-frequency modes significantly decreases to 84 meV in the crystal, occupying 21% of the total value. Due to the large suppression of EVC, the calculated k_{nr} decreases with four orders in magnitude from the isolated state to the crystal state. Hence, the emission efficiency of HPS can be boosted in the crystal state due to the restricted EVC.

Theoretically, the large EVC of most AIEgens is the main cause for their low emission efficiency in the isolated state, which originates from the nature of the conformational flexibility and high

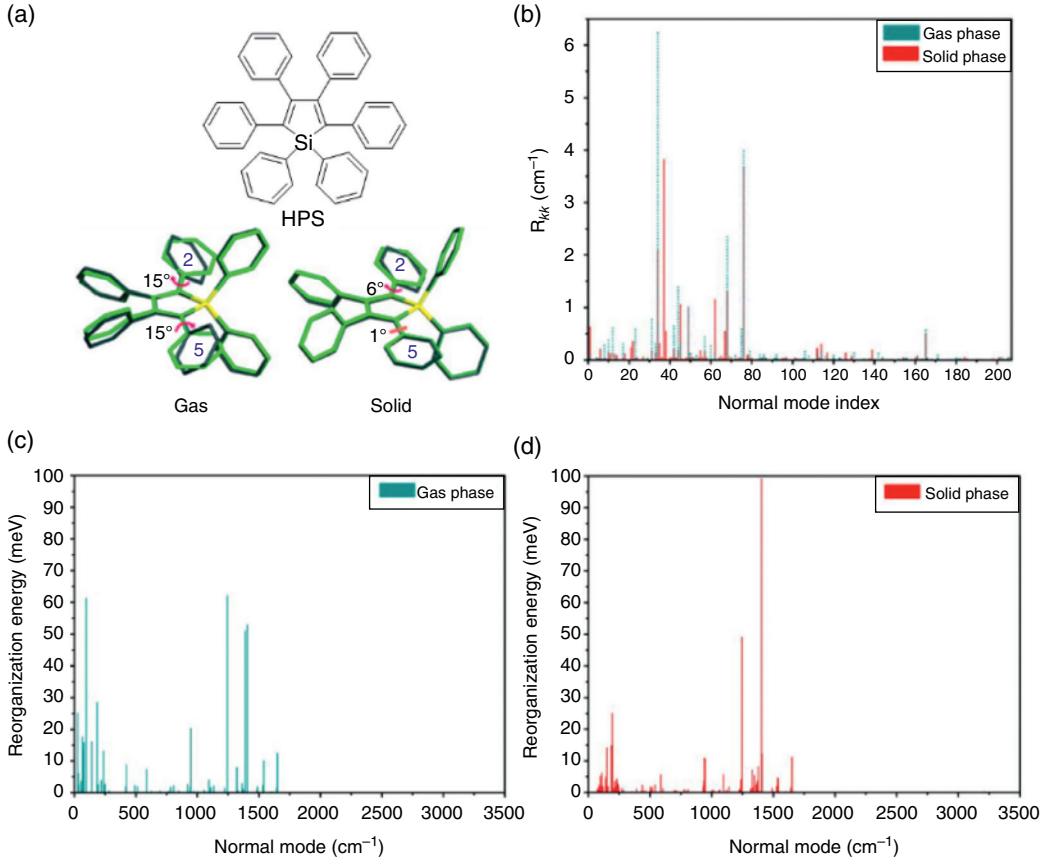


Figure 1.5 (a) Chemical structures and the overlap of the $S_{1,min}$ conformation and the $S_{0,min}$ conformation in the gas and the solid state of HPS. (b) Diagonal elements R_{kk} of the nonadiabatic electronic coupling matrix versus normal mode index in the gas and the solid state. (c) Reorganization energy versus normal mode wave numbers in the gas state and (d) the solid state. *Source:* Adapted from Ref. [7a] with permission from American Chemical Society.

freedom of molecular motions of the AIEgens. Tang and coworkers have studied the substituent effect on the AIE behaviors of a series of stilbene derivatives, as presented in Figure 1.6, and verified the influence from freedom of molecular motions on the excited-state properties [17b]. Three methyl groups can be attached to 2,4,5-positions or 2,4,6-positions of each phenyl rings of the stilbene, which leads to opposite photophysical behaviors. The 2,4,5-TMe-DPE shows aggregation-caused quenching effect, whereas the 2,4,6-TMe-DPE shows the typical AIE behavior. The first question that arises is which factors make the 2,4,5-substituted derivative highly emissive with Φ_F of 13.4% but the 2,4,6-substituted counterpart almost nonemissive with Φ_F as 0.6% in the dilute solution. The quantum simulations in the ground state show that 2,4,5-TMe-DPE owns a more planar conjugation plane, while 2,4,6-TMe-DPE is more twisted. The calculated rotation barrier shows that 2,4,6-TMe-DPE undergoes lower barrier to rotate along the coordinate of twisting, but it suffers higher barrier to move along the coordinate of planarization, which reveals that methyl groups in 4,6-positions can produce strong steric hindrance to prevent the coplanarization between phenyl rings and the double bond, but such steric hindrance can cause preliminary twisting of phenyl rings and reduce the conjugation degree, which leads to the easier torsional motions of the

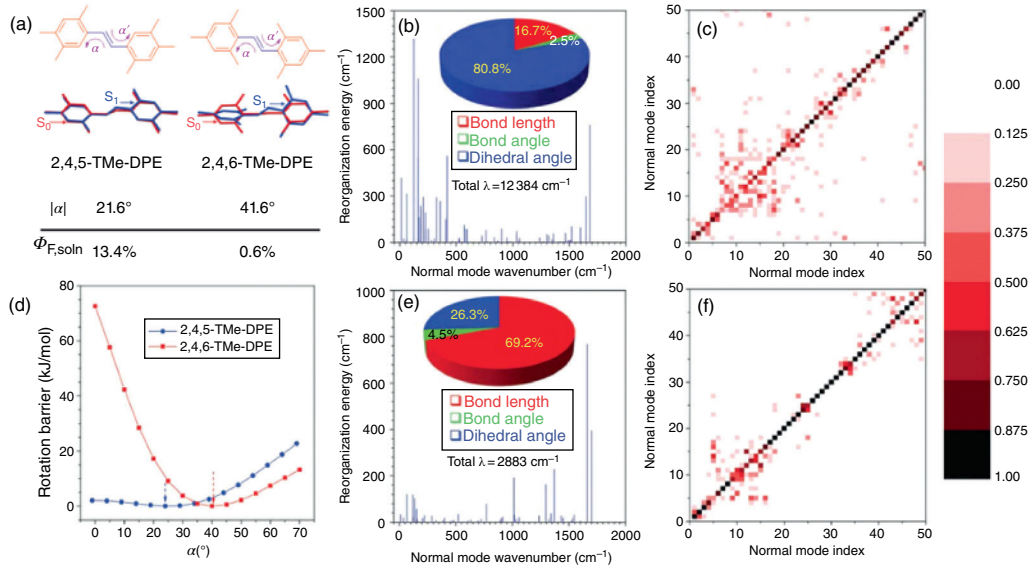


Figure 1.6 (a) Chemical structures, the overlaps of the $S_{1,min}$ conformation and the $S_{0,min}$ conformation in the gas phase, and fluorescence quantum yield in the dilute solution of 2,4,5-TMe-DPE and 2,4,6-TMe-DPE. Reorganization energy versus normal mode wave numbers in (b) the gas state and (e) the solid state of 2,4,6-TMe-DPE. Duschinsky rotation matrix of normal modes with index of 1–50 in (c) the gas state and (f) the solid state of 2,4,6-TMe-DPE. (d) Rotation barriers calculated through rotating the dihedral angle α. *Source:* Adapted from Ref. [17b] with permission from The Royal Society of Chemistry.

phenyl rings in 2,4,6-TMe-DPE. From the ultrafast spectroscopy measurement, the lifetime of excited-state species of 2,4,6-TMe-DPE is only 2.1 ps, much shorter than that of 2,4,5-TMe-DPE (263 ps), which indicates that the 2,4,6-TMe-DPE is less conjugated and possesses higher motion ability, so it can undergo much faster excited-state decay process.

Further EVC analysis is also consistent with the abovementioned result. The low-frequency molecular motions dominate in isolated 2,4,6-TMe-DPE, which are mainly associated with torsion of the phenyl rings and twisting of the double bond in the excited state. Projection of RE onto the internal coordinate shows that over 80% of the total RE comes from the change in dihedral angles, which further verifies the higher twisting mobility of 2,4,6-TMe-DPE. The calculation of the Duschinsky rotation matrix (DRM) shows that the mixing of low-frequency molecular motion modes of 2,4,6-TMe-DPE is much stronger than that of 2,4,5-TMe-DPE. The large area of nondiagonal elements on DRM indicates that 2,4,6-TMe-DPE owns multiple coupled decay pathways, connecting the excited-state state with the ground state, through molecular motions, that can further enhance the nonradiative decay rate. On the contrary, the highly emissive 2,4,5-TMe-DPE shows much less RE and less mixed motion modes. In the crystal state, the RE of 2,4,6-TMe-DPE decreases to a large extent and the light emission is brightened. The abovementioned analysis draws a clear mechanistic picture of the AIE effect that high freedom of the isolated AIE molecule generates dominant low-frequency molecular motions, rendering the excited-state energy mainly dissipated through the nonradiative pathways; meanwhile, the intensive low-frequency molecular motions can cause mixing among the motion modes, making the multiple decay pathways coupled together so that the nonradiative decay is further facilitated. These two factors cause the weak emission of AIEgens in the dilute solution. The low-frequency molecular motions can be drastically restricted in the solid state due to their higher sensitivity to the environmental constraints, so

the EVC can decrease to a large extent, leading to the decrease in the nonradiative decay rate, and then the luminescence quantum efficiency can be significantly boosted.

With persistent effort, researchers have revealed the importance of molecular motions to the luminescence process and triggered the experimental and theoretical studies on the molecular motions, and then, finally, they have concluded RIM, or theoretically the restriction of EVC, as the general working principle for AIE effect. RIM works well for explaining AIE behaviors for most AIEgens and serves as an effective design principle for the development of AIE materials. Recently, theoreticians have further explored specific features of PES in the excited states of AIEgens, considering the crossing between the excited state and the ground state and the coupling among the excited states.

1.3 Restricted Access to Conical Intersection

Previous experimental studies of molecular motions and theoretical analysis of EVC have elucidated the decay pathways of AIEgens, considering the starting and final equilibrium points on the first excited state and the ground state, respectively. Recently, theoreticians have investigated the dynamic features for both the excited state and the ground state of typical AIEgens by scanning the PES along specific molecular motion coordinates or by employing excited-state molecular dynamics method, which has presented a clear mechanism picture of the photoinduced dynamic evolution for AIEgens [18].

When we look into the NAC between the two equilibrium points on the excited state and the ground state, based on the displacement harmonic approximation, it is the intensive low-frequency modes that contribute to the energy conversion from the electronic form to the vibrational form. However, the massive molecular motions of a series of AIEgens can lead the excited-state structures to evolve beyond the assumption of harmonic approximation to form highly twisted structures. In such cases, the conical intersections (CIs) between the excited state and the ground state will become the main cause for the fast nonradiative decay or channels for photochemical reactions [18a].

Taking the dimethyl tetraphenylsilole (DMTPS) as the model compound [18b], the central silole ring can undergo the alternation of the C=C double bond after absorption of photons, which further promotes its motion ability in the excited state. The potential energy profiles of the DMTPS in the excited state optimized by CASPT2//CASSCF method (Figure 1.7b) show that the vibrational relaxation leads to a minimum point in the S_1 state with 3.1 eV, at which the central silole ring still keeps planar, whereas along with the twisting of the silole ring, the potential energy profile experiences an energy barrier at 3.54 eV and, finally, leads to a CI point at 3.0 eV between the S_1 and the S_0 state, at which the silole ring turns into a highly twisted conformation, similar to the structural reorganization of the cis-butadiene. Since the energy barrier separating the CI and the Frank–Condon region is lower than the vertical excitation energy, the CI is energetically accessible. Once the excited DMTPS species reach the CI, the NAC becomes infinitely large and finally results in the ultrafast nonradiative decay from the S_1 state to the S_0 state to quench the emission in the solution. But in the crystal, the QM/MM calculation of the potential energy profile shows that the CI is located at 4.91 eV, which is much higher than the vertical excitation energy of 3.65 eV, making the CI energetically inaccessible. Hence, the nonradiative decay through CI can be effectively blocked to recover the strong light emission.

When taking the dynamic evolution along the PES into consideration, it can be found that the TPE derivatives also have abundant decay pathways in the excited state, including both

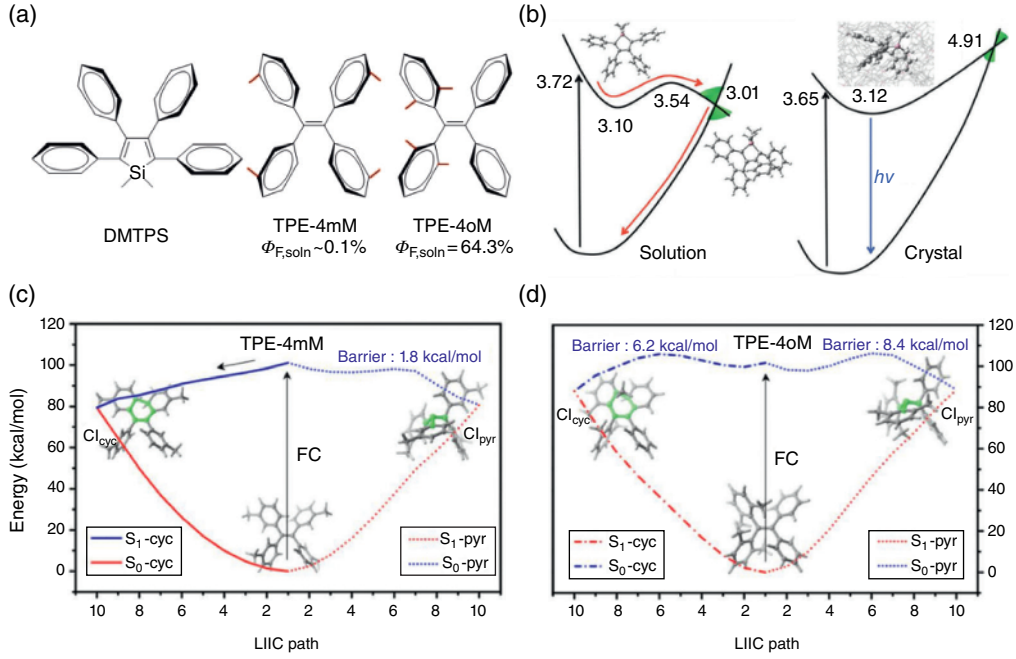


Figure 1.7 (a) Chemical structures and fluorescence quantum yield in the dilute solution of DMTPS, TPE-4mM, and TPE-4oM. (b) Schematic illustration of the potential energy profiles of DMTPS in the cyclohexane and the crystal. The potential energy profile in the cyclohexane is optimized at the CASSCF/6-31G (d) level with the PCM model. The vertical excitation energy for each point is recalculated using CASPT2 with the ANO-S basis set contracted to Si[4s3p1d]/C[3s2p1d]/H[2s1p]. The calculation in the crystal is performed by using ONIOM(CASSCF/6-31G(d):UFF) model with recalculating the QM energy by CASPT2. *Source:* Adapted from Ref. [18b] with permission from The Royal Society of Chemistry. Linear interpolation in internal coordinates paths calculated by using the OM2/MRCI method of (c) TPE-4mM and (d) TPE-4oM. *Source:* Adapted from Ref. [8a] with permission from American Chemical Society.

photophysical processes and photochemical reactions [8]. The excited-state molecular dynamics simulation for 1.5 ps based on the trajectory surface hopping (TSH) model shows that 75% of the simulated trajectories decay to the ground state through a CI and form the cyclization product with a new C–C single bond between the two adjacent phenyl rings. The distance between the two carbons is only 2.0 Å at the cyclization CI. There is 5% of the trajectory decay through the twisting of the C=C double bond. Similar decay features have been found in two TPE derivatives substituted with methyl groups at meta and ortho positions. The scanning of the linear interpolation in internal coordinates (LIIC) path using the OM2/multireference configuration interaction (MRCI) method is presented in Figures 1.6d and 1.7c.

Upon photoexcitation, TPE-4 mM can decay through the CI of cyclization with a negligible barrier, which is consistent with the TSH simulation that 88% of the total 558 trajectories drops into the ground state along the cyclization direction. On the other hand, there is only a relatively small barrier of 1.8 kcal/mol between the FC region and the CI for *E*/*Z* isomerization, which indicates TPE-4mM will undergo ultrafast nonradiative decay so that it is almost nonemissive in the solution. On the contrary, for the TPE-4oM with the methyl groups substituted at the ortho position of the phenyl rings, there are two notable barriers on both the cyclization and isomerization pathways, connecting the FC region with the cyclization CI and

the isomerization CI, respectively. Hence, there is no decay for TPE-4oM to the ground state of the total 568 trajectories in the TSH simulation for 1 ps, which accounts for its higher emission efficiency in the solution.

With scanning the PES or simulating by the TSH method, we can find that vigorous molecular motions of the highly flexible AIEgens in the excited state can lead to the CIs between the excited state and the ground state. These CIs will result in enormous nonradiative decay rates or generate another photoinduced product. Furthermore, the crossing between the excited states can also strongly affect the photophysical behaviors of luminogens that will generate the transition forbidden dark states.

1.4 Restriction of Access to the Dark State

RIM serves as the most effective guideline for the design of AIE molecules. However, RIM requires a more detailed elaboration when it is applied to the heteroatom-containing AIEgens. On the one hand, the introduction of heteroatoms endows the luminogens versatile functions, whereas, on the other hand, it makes the excited-state features of the luminogens more complicated. First, introduction of heteroatoms, often, produces the electron-donating or -withdrawing effect, and then facilitates the mixing of the overlap-forbidden charge-transfer (CT) state with the local-excited (LE) state. Second, heteroatoms with lone-pair electrons can import the crossing between the overlap-forbidden (n,π^*) state with the (π,π^*) state. What is more, (n,π^*) state will facilitate the intersystem crossing from the singlet states to the triplet states, which are spin forbidden and can be easily quenched. All these overlap-forbidden and spin-forbidden states have been defined as dark states that are detrimental to the fluorescence process [19].

Taking the (9-anthrylmethyl) bis(2-pyridylmethyl) amine (APA) as an example (Figure 1.8) [9], the APA only contains a large π-conjugation plane consisting of the anthracene and a triple-pyridine motif, but it shows the unique AIE property, which differs from typical AIEgens, usually, with multiple rotors. Although the APA contains the anthracene with large conjugation, it shows weak UV emission with a Φ_F of 0.6% in the dilute tetrahydrofuran (THF) solution with vibronic peaks. After chelation with the zinc ion, it shows enhanced emission with the Φ_F of about 100% with the similar vibronic peaks. Meanwhile, with more than 90% water added into the pure solution of APA, the resulting APA aggregate shows a broad and red-shifted emission band with a peak at 461 nm. The APA crystal also shows a similar emission band at 492 nm. The large spectral variation between the dilute solution and the solid state indicates the mixing of excited states with different characteristics.

Indeed, with optimization of the first two excited states of the isolated APA involving the transition of the lone pair electrons, two kinds of excited-state features have been figured out. According to the transition characteristics, the two close-lying excited states are assigned as (π,π^*) state and (n,π^*) state, which are vibronically coupled by the molecular motions. The bright (π,π^*) min owns large oscillator strength and is responsible for the light emission, whereas the lower-lying (n,π^*) min has the oscillator strength nearly close to 0 and crosses the (π,π^*) state through the CI, which causes the quenching of the light emission. The key molecular motion connecting these two steady excited-state points is the rotating of the nitrogen-containing group. Hence, when chelating with the zinc ion, the lone pair electrons of the nitrogen atoms and the motion of the whole chelating group are blocked, which results in the elevation of the (n,π^*) state and recovering of the light emission from the bright (π,π^*) state. Similarly, the APA molecules in the crystal can pack tightly

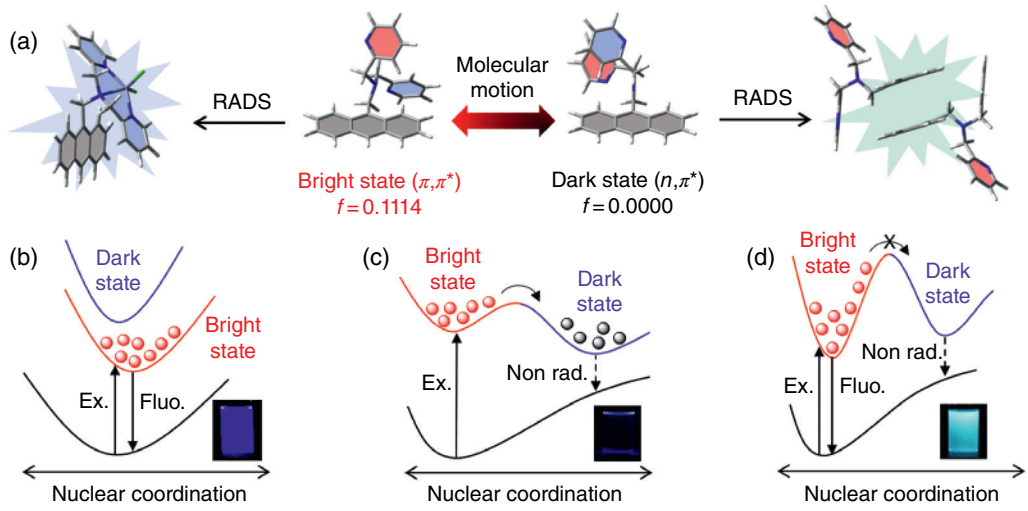


Figure 1.8 (a) Illustration of the coupling between the bright state and the dark state by the molecular motion, and the structures at the minimum points of the bright state and the dark state, the emissive chelation complex, and the dimer in the crystal. Schematic potential energy surfaces of RADS related to (b) the chelation with the zinc ion, (c) the dilute solution state, and (d) the dimers in the crystal.
Source: Adapted from Ref. [9] with permission from John Wiley and Sons.

to form dimers and stabilized by the intermolecular π–π interaction and multiple C–H interactions, which effectively hinder the rotation of the chelating groups. The lock of lone-pair electrons and motions of the nitrogen-containing group lead to the elevation of the dark (n,π^*) state and finally boost the fluorescence from the bright (π,π^*) state.

This mechanism can be concluded as the restriction of access to the dark state (RADS), which further elucidates the connotation of the RIM mechanism. The previous investigation mainly focuses on the NAC between the first excited state and the ground state. As an extreme scenario of NAC, the CI can cause ultrafast deactivation. In fact, the PES of multiple excited states can be coupled by molecular motions and arranged in a complicated manner, especially for the heteroatom-containing molecular systems. The accessible dark states like the CT state, (n,π^*) state, and the triplet state will cause the fluorescence quenching. Once the molecular motions that lead to the dark states undergo the intramolecular or environmental constraints, the fluorescence can be restored. The multistate model has been proved effective to evaluate the excited-state deactivation of the heteroatom-containing luminogens.

1.5 Suppression of Kasha's Rule

For classical luminophores, the internal conversions from higher excited states to the lowest excited states are much faster than the luminescence processes due to the rigid structures and large conjugation even in the gas phase or dilute solution, so the light emission always comes from the lowest excited state with a given spin multiplicity [20].

However, most AIEgens possess highly flexible structures with substantial low-frequency molecular motions that are sensitive to the environmental constraints. The vigorous molecular motions will contribute to the coupling and mixing of multiple excited states. Once the relevant molecular

motions are restricted in the aggregate or solid state, it is possible that the excitons can be stabilized in higher excited states and generate anti-Kasha light emissions.

Qian et al., first, proposed the suppression of Kasha's rule (SOKR) as the mechanism for the AIE behaviors of molecular rotors based on the boron-difluorohydrazone (BODIHY) [11a]. The luminescence properties related to higher excited states of the BODIHY derivatives in the solution have been studied through the spectroscopy by changing the viscosity of the solution and varying the excitation wavelength. These derivatives show viscosity-dependent emission enhancement but nearly no response to the solution polarity due to weak partial charge transfer. According to the calculation at the TDA-PBE level, the first excited state is designated as a dark state. Instead, the S_3 state is a bright state, which is more populated due to the relatively large energy gap between the S_3 and lower excited states. It is demonstrated that once the viscosity increases, the rotation of the phenyl rings can be hindered and make the excitons stabilized in the higher excited state to generate enhanced anti-Kasha emission. However, these results still remain controversial. Zhou et al. have recently employed more DFT functions to recheck the excited-state properties of the BODIHY derivatives and have challenged the SOKR mechanism [11b]. They have found that the TDA-PBE method used in Ref. [11a] may not describe the correct order of the excited states, and the energy gaps between S_3 and S_2 states obtained from this method are small enough to generate efficient internal conversion from S_3 and S_2 states. Hence, the emission of BODIHY derivatives in higher viscosity may not be induced by the SOKR. Instead, they proposed that the restriction of access to the CI caused by the flip-flop motion is responsible for the AIE behaviors of BODIHY derivatives.

Guo et al. has recently reported another luminogen named DMF-BP-PXZ with highly efficient light emission from the S_2 state (Figure 1.9a, b) [11c]. According to the calculation, the S_1 state is a transition-forbidden dark state, and the internal conversion dominates the decay process in the solution due to the severe molecular motions, so the rapid internal conversion from S_2 to S_0 state, through the intermediate S_1 state, quenches the light emission. However, its k_{IC} from S_2 to S_0 can be suppressed by four orders of magnitude, and the fluorescence radiation rate can be enhanced in the solid state, which leads to the efficient light emission from S_2 state to the ground state. In this regard, further experimental evidence for the stable population of higher excited states is still highly desired to solidify the claim on the anti-Kasha emission, but the mechanism demonstrated earlier also belongs to the category of RIM, and it validates the wide reliability of the RIM mechanism.

Exciton population on the higher excited states can also occur in the triplet states. Taking the ClBDBT as an example (Figure 1.9c, d), it exhibits white-light emission under UV light and persistent yellow afterglow in the room temperature [11d]. According to the calculated energy levels, T_1 and T_2 states are all lower than the S_1 state in energy, which makes both T_1 and T_2 accessible for the exciton population coming from the S_1 state. Furthermore, the T_2 state mainly contains the (n,π^*) transition character, which leads to a larger spin–orbit coupling (SOC) between T_2 and the S_0 and a higher radiative decay rate, whereas the T_1 state contains more (π,π^*) transition character. At room temperature, the small energy gap between T_2 and T_1 can promote the thermal population from T_1 to T_2. According to Boltzmann distribution, T_2 has a smaller population than T_1, but the faster radiative decay from T_2 results in a balanced emission intensity from both T_2 and T_1 states. Thus, the combined anti-Kasha blue light from T_2 and the yellow light from T_1 generate the efficient white-light emission at room temperature.

In fact, it is also the RIM process in the crystal state that stabilizes the specific electronic structures of T_2 and T_1 and restricts the nonradiative decay from triplet states to the ground state, and then the balanced dual emission can be restored.

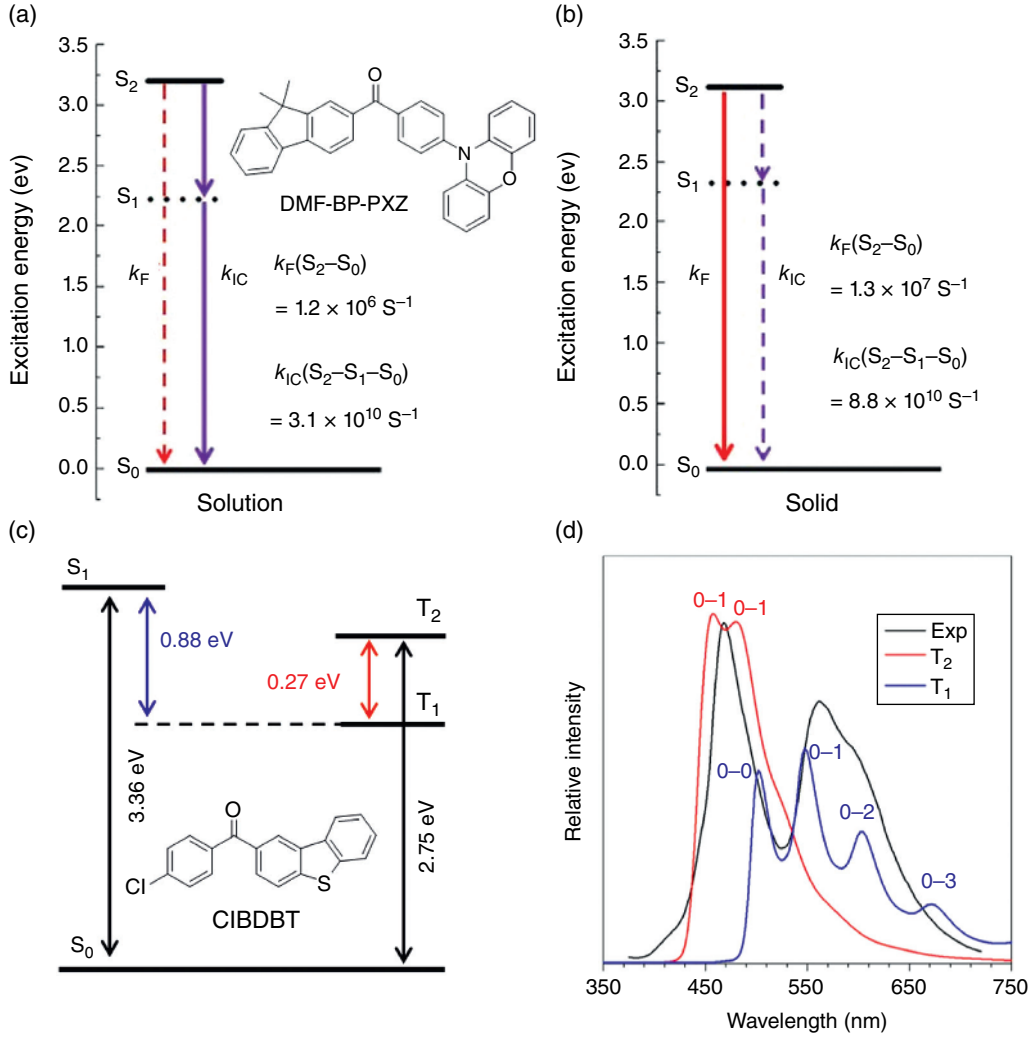


Figure 1.9 Molecular structure, calculated energy levels, fluorescence, and internal conversion rate constants of DMF-BP-PXZ in the (a) solution and (b) solid state. *Source:* Adapted from Ref. [11c] with permission from John Wiley and Sons. (c) Molecular structure, calculated energy levels, and (d) emission spectra of ClBDBT in the solid state. *Source:* Adapted from Ref. [11d] with permission from Springer Nature.

1.6 Through Space Conjugation

Most of the classical AIEgens are constructed by chromophores with through-bond conjugation (TBC), and their emission can be enhanced through restricting the nonradiative decay driven by molecular motions, whereas the light emission can also be boosted by promoting the radiative rates through the through-space conjugation (TSC) [13]. The TSC plays a key role in radiative decay processes of molecular systems with clusterization-triggered emission (CTE) property [21]. Moreover, a certain degree of molecular motions in the solid state will facilitate the intra- or intermolecular excited-state TSC for the nonconjugated molecules and stabilize the radiative channels and, thus, promote the emission intensity [13].

1.6.1 Clusterization-Triggered Emission

Traditional luminogens, generally, consist of aromatic groups or other conjugated building blocks and take the two-dimensional conjugated structure connected by chemical bonds. In such molecular systems with TBC, the EVC between emissive states and the ground state, the access to CIs, or the dark states driven by molecular motions are usually the detrimental causes for emission quenching. However, researchers have discovered and developed a nonconventional type of luminogens without any long-range conjugated structures but containing only isolated units such as heteroatoms with lone-pair electrons, unsaturated C=C, C=O, and C≡N groups as presented in Figure 1.10. Although this kind of luminogens lacks luminescent centers intuitively, and they are almost nonemissive in the dilute solution, they can emit visible light efficiently in the aggregate or solid state, showing the typical AIE behaviors. Because of the lack of largely conjugated luminescent centers and much higher motion ability than the traditional molecules with long-range conjugation, such nonconjugated molecules are nonemissive in the isolated state. However, it can be noticed that these heteroatom-containing groups usually exist as amide, imide, ketone, anhydride, or ester subunits connected by the saturated bonds in the macromolecule backbones, and they are usually rich in electrons. Hence, once the aggregation or cross-linking occurs, electron-rich moieties can cluster together and form a relatively stable long-range through-space electron ocean and energy bands by the electron overlapping for the electronic transition, which is similar to the energy band structures in the inorganic semiconductors. Upon excitation, electrons can jump into the excited state based on the stabilized through-space energy bands and light up the whole cluster system.

Such nonconventional phenomenon has been coined as CTE; it deciphers that the severe molecular motions and nonconjugated structures make the CTE luminogens nonemissive in the isolated state or the dilute solution, whereas diverse intra- and intermolecular interactions in the cluster or cross-linking can hamper the molecular motions and stabilize the conformations with large electron overlapping and thus boost the light emission of CTE luminogens, in which the packing density and the cluster size can affect the emission efficiency [21]. Taking the polyacrylonitrile

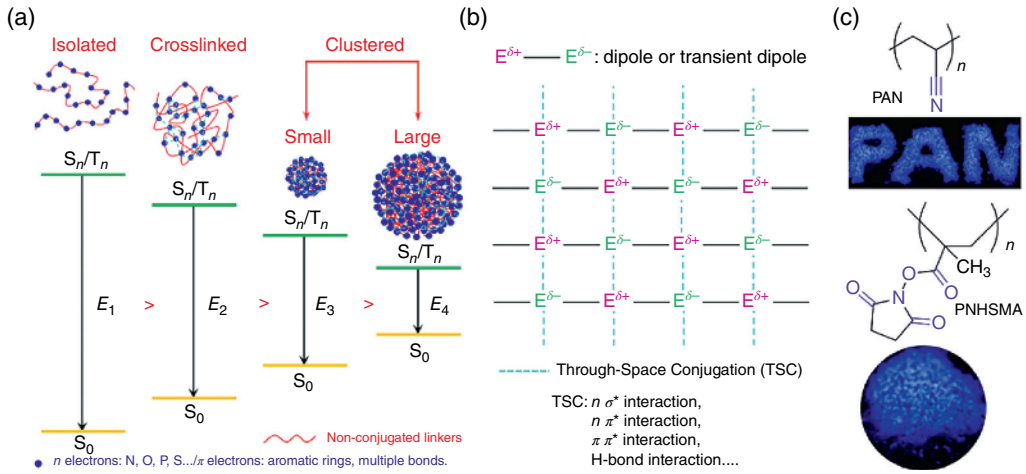


Figure 1.10 (a) Schematic illustration of the cluster formation, energy variation, and (b) the formation of through-space conjugation involved in the CTE. *Source:* Adapted from Ref. [21a] with permission from Elsevier. (c) Examples of CTEgens. *Source:* Adapted from Ref. [21b] with permission from John Wiley and Sons.

(PAN) [21b] and poly(*N*-hydroxysuccinimidyl methacrylate) (PNHSMA) [21c] as the example, they contain no aromatic groups and are nonconjugated in the isolated polymer backbone (Figure 1.10c). Therefore, these two molecules are nearly nonemissive in the dilute solution. But they can emit strong blue light in the concentrated solution or solid powder. CTE phenomenon also exists in the natural products such as starch, cellulose, and protein; they can show notable blue light in the solid state under UV excitation [21d].

1.6.2 Polymerization-induced Emission

Recently, Tang and coworkers have proposed polymerization-induced emission (PIE), which is another conceptual innovation related to CTE [22]. It describes the process where the nonemissive monomers can be converted into luminescent polymers through polymerization. AIE process occurs mainly by physically manipulating the molecular motions, whereas PIE is achieved through the chemical ways accompanied by the CTE process. As versatile polymerization methods can be utilized to construct the PIE polymers, and these unusual luminescent polymers own good processability, the PIE acts as a promising solution in developing novel soft luminescence materials.

The working principle underneath is similar with CTE, nonconjugated subunits with rich electrons, such as phenyl, hydroxyl, and carbonyl groups, ether, and amide, can be connected into polymer chains by chain polymerization or step polymerization, and such polymer chains can be entangled and form multilevel structures through diverse intra- or interchain motions. Then, the electron-rich moieties will aggregate into a cluster with electron overlapping in multiple microstructures and finally generate visible light. The emission intensity of the PIE polymers will increase with promoting the polymerization degree and the molecular weight. The intrinsic diverse structures endow the PIE polymers the potential to create diverse luminescence performance.

1.6.3 Excited-state Through-space Conjugation

From the abovementioned discussion, molecular motions are mainly detrimental to luminescence. Tang and coworkers have recently revealed a new role of molecular motions in the excited-state deactivation process of the tetraphenylethane (*s*-TPE) derivatives as presented in Figure 1.11a and b [13a].

The *s*-TPE only contains four phenyl rings connected by the saturated single bond but can intensely emit visible light with the peak at 467 nm in the solid state. The dilute solution of *s*-TPE shows ultraviolet emission that basically stems from the isolated phenyl rings, but with adding more than 70% water into the dilute solution, *s*-TPE molecules can aggregate accompanied with a notable emission peak at 460 nm emerging, showing the typical AIE property. Why do the nonconjugated systems emit the visible light? Due to the highly twisted and flexible structure of *s*-TPE, it shows no obvious intermolecular π–π interaction in the single crystal. The theoretical simulation of the exciton coupling also shows that there is no notable intermolecular coupling in the excited state, so it should be the intramolecular interaction that affects the emission.

Further optimization of the excited-state structures shows that *s*-TPE will encounter substantial conformational reorganization, and during the relaxation, the distance between the geminal phenyl rings can gradually decrease. When it decays to the $S_{1,min}$, two geminal phenyl rings reach a close-contacting conformation with large through-space overlapping of π orbitals. Indeed, the transition energy gaps decrease along with the phenyl rings getting close, so the emission wavelengths can be redshifted with such intramolecular motions. Finally, the calculated emission at $S_{1,min}$ becomes 460 nm, which is well consistent with the experimental data. The EVC analysis

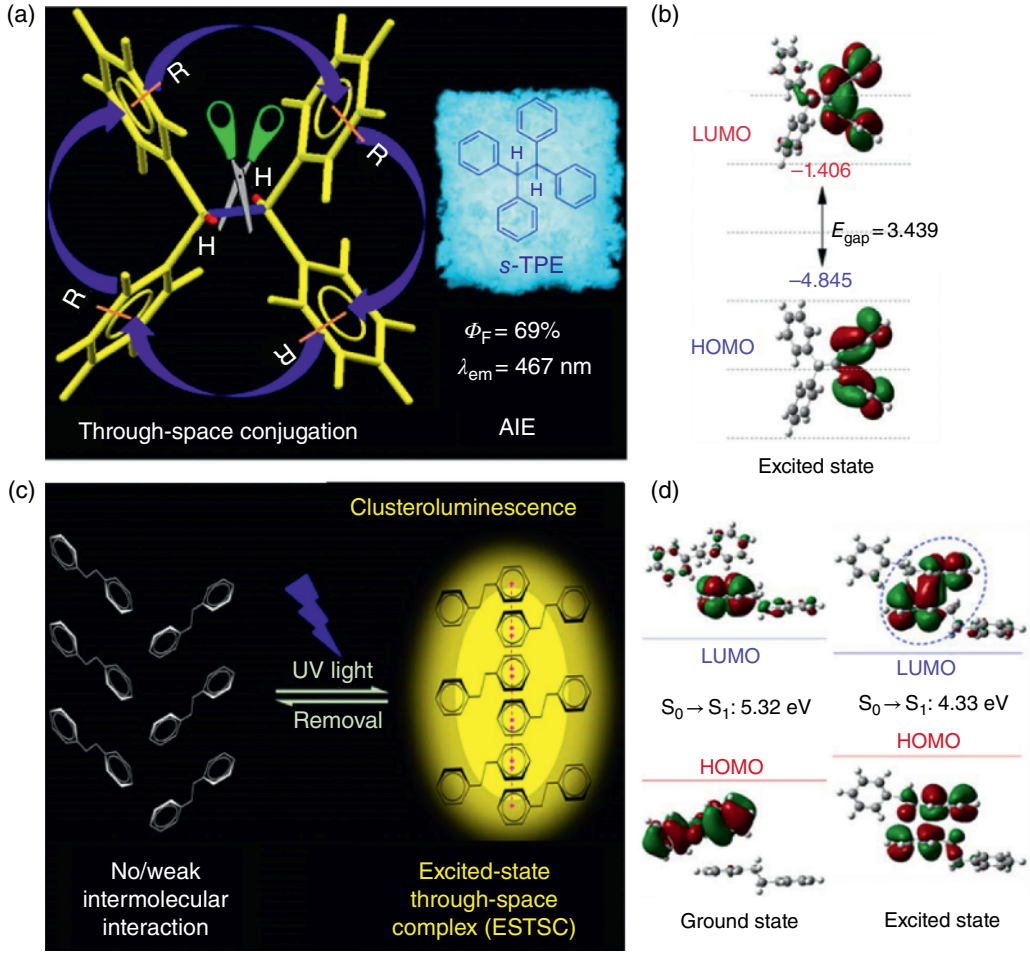


Figure 1.11 Schematic illustration of the excited-state (a) intramolecular through-space conjugation of *s*-TPE and (c) intermolecular through-space complex of *s*-DPE. Molecular orbitals involved in the transition between the excited state and the ground state of (b) *s*-TPE and (d) *s*-DPE. *Source:* Adapted from Refs. [13a, b] with permission from American Chemical Society.

shows that *s*-TPE molecules own much higher excited-state motion ability in the dilute solution, so the conformation with intramolecular TSC can be easily disturbed by the vigorous molecular motions. Once the *s*-TPE molecules aggregate, the molecular motions will be restricted to a certain degree, as indicated by the suppressed structural reorganization, which, thus, stabilizes the through-space conjugated conformation and reduces the nonradiative decay rates, and so the solid-state *s*-TPE can emit enhanced visible light.

A certain degree of molecular motions in the solid state will facilitate the formation and stabilization of emissive states with TSC. The diphenylethane (*s*-DPE) is another nonconventional AIEgen as presented in Figure 1.11c and d [13b]. It contains no long-range through-bond conjugated structure but two isolated phenyl rings. The absorption and photoluminescence spectra in the dilute THF solution are ascribed to the electronic transition of the phenyl rings, with peaks at 270 and 285 nm, respectively. However, with addition of water into its dilute solution, a new emission peak at 355 nm gradually emerges, showing the AIE phenomenon. The emission peak in the

solid state of *s*-DPE is also redshifted to 355 nm with a small fraction of the emission at 285 nm coming from the isolated state. Different from *s*-TPE, the isolated *s*-DPE molecule cannot form the intramolecular TSC, so the only way to redshift the light emission is to form the intermolecular TSC. The optimization of the dimer of *s*-DPE based on two adjacent *s*-DPE molecules in the single crystal shows that the two *s*-DPE molecules gradually get closer and turn the orientation of two phenyl rings from face-to-edge at $S_{0,min}$ to face-to-face at $S_{1,min}$ and finally form an excited-state through-space complex (ESTSC) with significant orbit overlapping between the two respective phenyl rings of the two *s*-DPE molecules. Meanwhile, the energy gap decreases from 5.32 to 4.33 eV along with the light-driven solid-state intermolecular motions, which is the luminescence origin of *s*-DPE in the solid state.

As the characteristic ultrafast transient absorption spectra reveal the most probable conformations in the excited-state timescale, the femtosecond transient absorption (fs-TA) spectroscopy has been utilized to prove the existence of ESTSC [13b]. The steady-state absorption spectra of *s*-DPE in dilute solution and crystal film have been first measured, respectively. It has been found that the absorption spectra in these two conditions are matched with each other, indicating there are no species involving intermolecular electronic coupling in the ground-state crystal film. Then, the fs-TA spectra of *s*-DPE in the dilute solution show that there are no notable absorption peaks in the long-wavelength region in the excited state but only peaks located in the short-wavelength region. However, when it comes to the crystal state, the fs-TA spectra of *s*-DPE crystal film show that the peaks from 340 to 450 nm almost disappear, but new peaks at 590 nm emerge as the dominant characteristic absorption peaks with the lifetime of 525 ps, which is similar to a characteristic transient absorption peak at 570 nm for the literature-reported naphthalene excimer. According to the theoretical simulation, this long-wavelength characteristic peaks can be assigned to the ESTSC. Since the ground-state *s*-DPE crystal will not form complexes, the ESTSC can only be formed in the excited state along with the intermolecular motions.

What is the driving force for the molecular motions that lead to the formation of ESTSC? The Mulliken charges have been mapped onto molecular structures of the isolated *s*-DPE and the ESTSC [13b]. It shows that partial molecular charges of two carbon atoms of the isolated *s*-DPE connecting two phenyl rings and the central ethane moiety are negative, whereas the other carbon atoms show positive partial charges. Hence, it is proposed that such opposite partial charge distribution will induce the transient dipole to attract the adjacent two molecules approaching to each other and finally form a stable ESTSC. For the ESTSC, the partial charges of the two connection carbon atoms become even more positive.

CTE can be categorized as a kind of static clusteroluminescence, in which the aggregation restricts the molecular motions and stabilizes the emissive cluster. In contrast, ESTSC can be ascribed as dynamic clusteroluminescence, in which the excited-state molecular motions in solid state facilitate the formation of the key emissive cluster. The ESTSC opens a broad way to utilize the excited-state solid-state molecular motions for luminescence and offers a new design strategy for dynamic luminescence materials.

1.7 Perspective

Traditional photophysical research usually targets highly rigid and conjugated chromophores. However, investigation of the relationship between molecular motions with the excited-state decay process as well as manipulation of molecular motions in different manners and multiple states has been a consistent topic in the AIE mechanistic research [23]. From tremendous experimental and

theoretical contributions, RIM has been concluded as the general working principle, or the restriction of EVC in the quantum view [6, 7]. AIEgens own high performance in the aggregate or solid state that can hamper the internal conversion between excited states, in which the Kasha's rule may be invalid [11]. In light of this, the multistate mechanistic model, involving emissive excited states and transition-forbidden states, has offered perspectives in exploring the nature of higher excited states in the AIE process. In fact, multiple excited states can be involved in the photophysical process of AIEgens, especially for the heteroatom-containing systems. The proximity effect between the excited states with different property tends to induce the mixing of the states and finally leads to the crossing between dark states (CT, (n, n*), triplet states, etc.) and bright states [19]. The aggregate effect can render repopulation of the excited species, which may make the photophysical processes more complicated than those predicted by the classical luminescence theories [9]. Furthermore, the current RIM mechanistic model mainly focuses on the single-molecule property, whereas the surrounding molecules serve as the environmental constraint. Hence, more accurate and general theoretical models for the aggregate are still highly desired that consider adequate multistate properties and diverse intermolecular interactions.

Recently, research on the CTE has substantially expanded the mechanistic scope into the aggregate science, that the efficient light emission can be achieved through the clusterization of nonconjugated subunits [21]. Although the power source of CTE is mainly ascribed to the electronic overlapping among electron-rich moieties, the specific cluster structures remain unclear and only at the simulation stage as well as the specific interaction involving in the electronic transition of CTEgens, so reliable experimental characterization of the cluster structures and more accurate molecular dynamics simulation are highly demanded. In the sense that the clusterization in the ground state or the excited state will lead to electronic transition and boost radiative decay rates, CTE has opened a new broad way for luminescence research in the mesoscale. It is also likely to lead to the fusion of the organic luminescence theory with the inorganic band theory in CTE research.

From the traditional rigid chromophores to flexible AIEgens, and from classical AIEgens with TBC to nonconventional CTEgens with TSC, the mechanistic studies on luminescence have been evolving forward step by step. The study on the excited-state TSC has unveiled the mysteries of dynamic emissive states, driven by the excited-state molecular motions in the solid state [13]. Indeed, the intermolecular motions can also influence the luminescence process. On the one hand, the light-driven solid-state intermolecular motions contribute to the formation of ESTSC for nonconjugated luminogens. On the other hand, they can also be detrimental to the intermolecular emissive species and cause kinetic quenching. In this sense, the research of molecular motions can be expanded into multiple intermolecular motions.

From the abovementioned cases, a certain degree of solid-state molecular motions can do advantageous work. This effect can be further demonstrated in the Herzberg–Teller (HT) effect [12], in which the vibronic coupling will facilitate the electronic transition, as well as the spin-vibronic coupling (SVC) for intersystem crossing process [24]. The HT effect describes that the electronic transition will be forbidden if the lowest excited states are dark states. However, with specific motion degrees, the interaction between electronic and vibrational motions can help to compensate for the transition dipole moment through specific vibration modes and facilitate the radiative transition. Such radiative enhancement has not been investigated for solid-state AIEgens, which may help to open another mechanistic research topic based on aggregate science. For most organic room-temperature phosphorescence (RTP) systems, increasing the SOC and restricting the nonradiative decay are the two main ways to enhance RTP efficiency. In this regime, the internal conversion driven by NAC associated with the molecular motions and the intersystem crossing driven by the SOC are always discussed separately due to the largely different timescale for these processes to take effect. In fact, the vigorous molecular motions can cause strong mixing among excited

states, in which the NAC and the SOC will present simultaneously. Hence, for evaluating the intersystem crossing process, the electron, spin, and vibration should all be considered in spin–vibronic levels [24]. The discussion on the HT effect shows that a specific vibrational degree of freedom is required to activate the HT transition. Similarly, the SOC is not always limited to a specific configuration. The higher-order terms depending on the molecular vibrations in the SOC expression will have significant contributions to the total SOC and finally facilitate the intersystem crossing. In this sense, representative molecular models can be designed to explore the SVC mechanism for organic RTP systems and finally make efficient use of the molecular motions.

References

1 (a) Kassem S, Leeuwen T, Lubbe AS, et al. Artificial molecular motors. *Chem Soc Rev* 2017; 46: 2592–2621; (b) Leeuwen T, Lubbe AS, Štacko P, et al. Dynamic control of function by light-driven molecular motors. *Nat Rev Chem* 2017; 1: 0096; (c) Erbas-Cakmak S, Leigh DA, McTernan CT, et al. Artificial molecular machines. *Chem Rev* 2015; 115: 10081−10206.

2 Turro NJ, Scaiano JC and Ramamurthy V. *Modern molecular photochemistry of organic molecules*. University Science Books, 2010.

3 (a) Shuai Z and Peng Q. Organic light-emitting diodes: theoretical understanding of highly efficient materials and development of computational methodology. *Natl Sci Rev* 2017; 4: 224−239; (b) Shuai Z and Peng Q. Excited states structure and processes: understanding organic light-emitting diodes at the molecular level. *Phys Rep* 2014; 537: 123−156.

4 Forster T and Kasper K. Ein Konzentrationsumschlag der Fluoreszenz. *Zeitschrift für Physikalische Chemie* 1954; 1: 275−277.

5 Luo J, Xie Z, Lam JWY, et al. Aggregation-induced emission of 1-methyl-1,2,3,4,5-pentaphenylsilole. *Chem Commun* 2001; 18: 1740−1741.

6 (a) Mei J, Leung NLC, Kwok RTK, et al. Aggregation-induced emission: together we shine, united we soar! *Chem Rev* 2015; 115: 11718−11940; (b) Mei J, Hong Y, Lam JWY, et al. Aggregation-induced emission: the whole is more brilliant than the parts. *Adv Mater* 2014; 26: 5429−5479; (c) He Z, Ke C and Tang BZ. Journey of aggregation-induced emission research. *ACS Omega* 2018; 3: 3267−3277; (d) Chen Y, Lam JWY, Kwok RTK, et al. Aggregation-induced emission: fundamental understanding and future developments. *Mater Horiz* 2019; 6: 428−433; (e) Zhao Z, Zhang H, Lam JWY, et al. Aggregation-induced emission: new vistas at the aggregate level. *Angewandte Chemie Int Edn* 2020; 59: 2−22.

7 (a) Zhang T, Jiang Y, Niu Y, et al. Aggregation effects on the optical emission of 1,1,2,3,4,5-Hexaphenylsilole (HPS): a QM/MM study. *J Phys Chem A* 2014; 118: 9094−9104; (b) Zhang T, Peng Q, Quan C, et al. Using the isotope effect to probe an aggregation induced emission mechanism: theoretical prediction and experimental validation. *Chem Sci* 2016; 7: 5573−5580; (c) Zhang T, Ma H, Niu Y, et al. Spectroscopic signature of the aggregation-induced emission phenomena caused by restricted nonradiative decay: a theoretical proposal. *J Phys Chem C* 2015; 119: 5040−5047; (d) Wu Q, Deng C, Peng Q, et al. Quantum chemical insights into the aggregation induced emission phenomena: a QM/MM study for Pyrazine derivatives. *J Comput Chem* 2012; 33: 1862−1869; (e) Peng Q, Yi Y, Shuai Z, et al. Toward quantitative prediction of molecular fluorescence quantum efficiency: role of Duschinsky rotation. *J Am Chem Soc* 2007; 129: 9333−9339; (f) Niu Y, Li W, Peng Q, et al. Molecular materials property prediction package (MOMAP) 1.0: a software package for predicting the luminescent properties and mobility of organic functional materials. *Mol Phys* 2018; 116: 1078−1090; (g) Niu Y, Peng Q, Shuai Z, et al. Promoting-mode free formalism for excited state radiationless decay process with Duschinsky rotation effect. *Sci China Ser B Chem* 2008; 51: 1153−1158.

8 (a) Gao Y, Chang X, Liu X, et al. Excited-state decay paths in tetraphenylethene derivatives. *J Phys Chem A* 2017; 121: 2572–2579; (b) Prlj A, Došlić N, Corminboeuf C, et al. How does tetraphenylethylene relax from its excited states? *Phys Chem Chem Phys* 2016; 18: 11606–11609.

9 Tu Y, Liu J, Zhang H, et al. Restriction of access to the dark state: a new mechanistic model for heteroatom-containing AIE systems. *Angewandte Chemie Int Edn* 2019; 58: 14911–14914.

10 (a) Bu F, Duan R, Xie Y, et al. Unusual aggregation-induced emission of a coumarin derivative as a result of the restriction of an intramolecular twisting motion. *Angewandte Chemie Int Edn* 2015; 54: 14492–14497; (b) Zhao Z, Zhen X, Du L, et al. Non-aromatic annulene-based aggregation-induced emission system via aromaticity reversal process. *Nat Commun* 2019; 10: 2952.

11 (a) Qian H, Cousins ME, Horak EH, et al. Suppression of Kasha's rule as a mechanism for fluorescent molecular rotors and aggregation-induced emission. *Nat Chem* 2017; 9: 83–87; (b) Zhou P, Li P, Zhao Y, et al. Restriction of flip-flop motion as a mechanism for aggregation-induced emission. *J Phys Chem Lett* 2019; 10: 6929−6935; (c) Guo J, Fan J, Lin L, et al. Mechanical insights into aggregation-induced delayed fluorescence materials with anti-Kasha behavior. *Adv Sci* 2019; 6: 1801629; (d) He Z, Zhao W, Lam JWY, et al. White light emission from a single organic molecule with dual phosphorescence at room temperature. *Nat Commun* 2017; 8: 416.

12 Herzberg G and Teller E. Schwingungsstruktur der Elektronenübergänge bei mehratomigen Molekülen. *Zeitschrift für Physikalische Chemie* 1933; 21: 410.

13 (a) Zhang H, Zheng X, Xie N, et al. Why do simple molecules with "isolated" phenyl rings emit visible light? *J Am Chem Soc* 2017; 139: 16264–16272; (b) Zhang H, Du L, Wang L, et al. Visualization and manipulation of molecular motion in the solid state through photoinduced clusteroluminescence. *J Phys Chem Lett* 2019; 10: 7077−7085; (c) Sturala J, Etherington MK, Bismillah AN, et al. Excited-state aromatic interactions in the aggregation-induced emission of molecular rotors. *J Am Chem Soc* 2017; 139: 17882–17889.

14 (a) Chen J, Lam CCW, Lam JWY, et al. Synthesis, light emission, nanoaggregation, and restricted intramolecular rotation of 1,1-substituted 2,3,4,5-tetraphenylsiloles. *Chem Mater* 2003; 15: 1535–1546; (b) Fan X, Sun J, Wang F, et al. Photoluminescence and electroluminescence of hexaphenylsilole are enhanced by pressurization in the solid state. *Chem Commun* 2008; 26: 2989−2991; (c) Li Z, Dong Y, Mi B, et al. Structural control of the photoluminescence of silole regioisomers and their utility as sensitive regiodiscriminating chemosensors and efficient electroluminescent materials. *J Phys Chem B* 2005; 109: 10061–10066; (d) Zhao E, Lam JWY, Hong Y, et al. How do substituents affect silole emission? *J Mater Chem C* 2013; 1: 5661−5668; (e) Liang GD, Lam JWY, Qin W, et al. Molecular luminogens based on restriction of intramolecular motions through host–guest inclusion for cell imaging. *Chem Commun* 2014; 50: 1725−1727; (f) Qin A, Lam JWY, Mahtab F, et al. Pyrazine luminogens with "free" and "locked" phenyl rings: understanding of restriction of intramolecular rotation as a cause for aggregation-induced emission. *Appl Phys Lett* 2009; 94: 253308.

15 Leung NLC, Xie N, Yuan W, et al. Restriction of intramolecular motions: the general mechanism behind aggregation-induced emission. *Chem A Eur J* 2014; 20: 15349–15353.

16 Cai Y, Du L, Samedov K, et al. Deciphering the working mechanism of aggregation-induced emission of tetraphenylethylene derivatives by ultrafast spectroscopy *Chem Sci* 2018; 9: 4662.

17 (a) Liu J, Pan L, Peng Q, et al. Tetraphenylpyrimidine-based AIEgens: facile preparation, theoretical investigation and practical application. *Molecules* 2017; 22: 1679; (b) Zhang H, Liu J, Du L, et al. Drawing a clear mechanistic picture for the aggregation-induced emission process. *Mater Chem Front* 2019; 3: 1143–1150; (c) Chen M, Hu X, Liu J, et al. Rational design of red AIEgens with a new core structure from non-emissive heteroaromatics. *Chem Sci* 2018; 9: 7829–7834; (d) Chen

M, Zhang X, Liu J, et al. Evoking photothermy by capturing intramolecular bond stretching vibration-induced dark-state energy. *ACS Nano* 2020; 14: 4265–4275.

18 (a) Crespo-Otero R, Li Q and Blancafort L. Exploring potential energy surfaces for aggregation-induced emission—from solution to crystal. *Chem Asian J* 2019; 14: 700–714; (b) Peng X, Ruiz-Barragan S, Li Z, et al. Restricted access to a conical intersection to explain aggregation induced emission in dimethyl tetraphenylsilole. *J Mater Chem C* 2016; 4: 2802–2810; (c) Li Q and Blancafort L. A conical intersection model to explain aggregation induced emission in diphenyl dibenzofulvene. *Chem Commun* 2013; 49: 5966–5968; (d) Sasaki S, Suzuki S, Sameera WMC, et al. Highly twisted N,N-dialkylamines as a design strategy to tune simple aromatic hydrocarbons as steric environment-sensitive fluorophores. *J Am Chem Soc* 2016; 138: 8194–8206.

19 (a) Liese D and Haberhauer G. Rotations in excited ICT states—fluorescence and its microenvironmental sensitivity. *Isr J Chem* 2018; 58: 813–826; (b) Grabowski ZR, Rotkiewicz K and Rettig W. Structural changes accompanying intramolecular electron transfer: focus on twisted intramolecular charge-transfer states and structures. *Chem Rev* 2003; 103: 3899–4031; (c) Lower S and El-Sayed M. The triplet state and molecular electronic processes in organic molecules. *Chem Rev* 1966; 66: 199–241; (d) Zgierski MZ, Fujiwara T and Lim EC. Role of the $\pi\sigma^*$ state in molecular photophysics. *Acc Chem Res* 2010; 43: 506–517.

20 Kasha, M. Characterization of electronic transitions in complex molecules. *Discuss Faraday Soc* 1950; 9: 14–19.

21 (a) Zhang H, Zhao Z, McGonigal PR, et al. Clusterization-triggered emission: uncommon luminescence from common materials. *Mater Today* 2020; 32: 275–292; (b) Zhou Q, Cao B, Zhu C, et al. Clustering-triggered emission of nonconjugated polyacrylonitrile. *Small* 2016; 12: 6586–6592; (c) Bin X, Luo W, Yuan W, et al. Clustering-triggered emission of poly (N-hydroxysuccinimide methacrylate). *Acta Chim Sin* 2016; 74: 935–941; (d) Gong Y, Tan Y, Mei J, et al. Room temperature phosphorescence from natural products: crystallization matters. *Sci China Chem* 2013; 56: 1178–1182; (e) Yuan W and Zhang Y. Nonconventional macromolecular luminogens with aggregation-induced emission characteristics. *Polym Chem* 2017; 55: 560–574.

22 Liu B, Zhang H, Liu S, et al. Polymerization-induced emission. *Mater Horiz* 2020; 7: 987–998.

23 Liu S, Li Y, Zhang H, et al. Molecular motion in the solid state. *ACS Mater Lett* 2019; 1: 425–431.

24 Penfold TJ, Gindensperger E, Daniel C, et al. Spin-vibronic mechanism for intersystem crossing. *Chem Rev* 2018; 118: 6975–7025.